ADVANCED MULTIVARIATE INVERSION TECHNIQUES FOR HIGH RESOLUTION 3D GEOPHYSICAL MODELING

Monica Maceira[1], Charlotte A. Rowe[1], Haijiang Zhang[2], Ryan T. Modrak[1], Michael L. Begnaud[1], Lee K. Steck[1], George R. Randall[1], and Xiaoning (David) Yang[1]

Los Alamos National Laboratory[1] and Massachusetts Institute of Technology[2]

Sponsored by the National Nuclear Security Administration

Award No. DE-AC52-06NA25396/LA09-3D Inv-NDD02

ABSTRACT

To meet the United States Government (USG) nuclear explosion monitoring (NEM) requirements with high confidence, the Air Force Technical Applications Center (AFTAC) needs new and improved capabilities for analyzing regional seismic, teleseismic, and infrasound event data. Recently, the National Nuclear Security Administration (NNSA) has decided to move toward 3D modeling to improve knowledge of the compressional and shear velocity structure and enable us to reduce uncertainty and more accurately detect, locate, and identify small (body wave magnitude m_b<4) seismic events. For seismically active areas, with good ground truth event coverage, inaccurate models can be corrected by interpolating results from nearby archived events (using the kriging methodology) and, therefore, it is possible to detect, locate, and identify large events even with limited resolution models. This is not necessarily the case for smaller events, however, and it is even more of a challenge for aseismic regions. On the other hand, focus on near-regional to local monitoring, demands that we address the Earth's heterogeneities and 3D complexities.

Motivated by the shortcomings of existing single-parameter inversion methods in accurate prediction of both seismic waveforms and other geophysical parameters, this research focuses on the development and application of advanced multivariate inversion techniques to generate a realistic, comprehensive, and high-resolution 3D model of the seismic structure of the crust and upper mantle that satisfies multiple independent geophysical datasets. Building on previous efforts, we have added a fourth dataset to the simultaneous joint inversion methodology. We present a 3D seismic velocity model of the crust and upper mantle of northwest China resulting from the simultaneous joint inversion of surface wave dispersion observations, teleseismic P-wave receiver functions, gravity anomalies, and body wave (P and S phases) travel times. Surface wave dispersion measurements are primarily sensitive to seismic shear-wave velocities. But, at shallow depths, it is difficult to obtain high-resolution velocities and to constrain the structure. This is because the longer the period, the deeper the surface wave energy penetrates, so shorter periods are primarily sensitive to upper crustal structures. Short periods are difficult to measure especially in tectonically and geologically complex areas. On the other hand, gravity inversions have the greatest resolving power at shallow depths because gravity anomalies decrease in amplitude and increase in wavelength with increasing depth. Gravity measurements also provide constraints on rock density variations. In addition, surface wave dispersion measurements are primarily sensitive to vertical shear-wave velocity averages; while body wave receiver functions are sensitive to shear-wave velocity contrasts and vertical travel-times. The addition of the fourth dataset consisting of seismic body wave travel-time data helps to constrain the seismic wave velocities both vertically and horizontally in the model cells crossed by the ray paths. An iterative, conjugate gradient-based least squares inversion is used to jointly model the four different data sets.

At the same time, we are testing different relationships between seismic velocities and density in a region in east Africa where we have obtained on-land Bouguer gravity measurements. These sensitivity studies will ensure the validity of the relations used in our 3D seismic imaging efforts.

OBJECTIVES

The ultimate goal of this study is to improve our knowledge of the 3D compressional and shear velocity structure and enable us to reduce uncertainty and more accurately detect, locate, and identify small (body wave magnitude m_b<4) seismic events, and therefore improve our capabilities for NEM. This project specifically improves seismic monitoring technology through the development and application of advanced multivariate inversion techniques to generate a realistic, comprehensive, and high-resolution 3D model of the seismic structure of the crust and upper mantle that satisfies numerous independent geophysical datasets.

RESEARCH ACCOMPLISHED

The characterization of the 3D continental structure is of fundamental importance to understanding crustal generation and its geodynamic evolution. Researchers from a variety of institutions have been investigating the idea of 3D geophysical modeling for decades. Inversion methods for determining the 3D velocity structure of the crust and mantle have been used since the late 70's (e.g., Aki et al., 1977). The so-called "cooperative inversion" defined by Lines et al. (1988) refers to the inversion of various, potentially different sets of geophysical observations, and can be formulated as a simultaneous inversion or as a sequential inversion. Joint inversion incorporates all the data sets simultaneously and in one data vector. This approach was followed by Lees and VanDecar (1991) to model seismic travel times and gravity data. On the other hand, sequential inversion treats each data set separately on alternating steps so the results of one inversion are used as the initial constraint for the next step. This approach was preferred by Lines et al. (1988) and Parsons et al. (2001) among others. The different data sets used in these "cooperative inversions" varied from resistivity and magnetotelluric data (Jupp and Vozoff, 1975), to teleseismic or local travel times and gravity data (Oppenheimer and Herkenhoff, 1981; Onizawa et al., 2002), to receiver function and surface wave dispersion observations (Julià et al., 2000; 2003; 2005), or to surface wave group and phase velocities (Villaseñor et al., 2001).

Maceira and Ammon (2006) were pioneers in implementing a method to jointly invert surface wave group velocities and free-air gravity observations. Inversion of surface wave dispersion data is a standard method for determining 3D shear velocity structure of the crust and upper mantle of the Earth. Nevertheless, it is well known that traditional state-of-the-art inversion techniques suffer from poor resolution and nonuniqueness, especially when a single surface wave mode is used (Huang et al., 2003). This is particularly true at shallow depths where the shorter periods, which are primarily sensitive to upper crustal structures, are difficult to measure especially in tectonically and geologically complex areas such as China and surrounding regions. On the other hand, gravity inversions have the greatest resolving power at shallow depths because gravity anomalies decrease in amplitude and increase in wavelength with increasing depth. Moreover, gravity measurements also supply constraints on rock density variations. Maceira and Ammon (2009) successfully applied this methodology to investigate the 3D shear velocity structure beneath the Tarim and Junggar basins in central Asia. Since then, LANL has been in the forefront of the development of joint inversion methods for high-resolution 3D modeling. During 2007 LANL researchers extended the surface wave/gravity inversion methodology to include P-wave teleseismic receiver functions (Rowe et al., 2007).

Method

Building on the mentioned previous efforts, we have added a fourth dataset to the simultaneous joint inversion methodology. The new 3D seismic velocity model of the crust and upper mantle results from the simultaneous joint inversion of surface wave dispersion observations, teleseismic *P*-wave receiver functions, gravity anomalies, and body wave (*P* and *S* phases) travel times. Surface wave dispersion measurements are primarily sensitive to vertical shear-wave velocity averages; while body wave receiver functions are sensitive to shear-wave velocity contrasts and vertical travel-times. Addition of the fourth dataset consisting of seismic body wave travel-time data helps to constrain the seismic wave velocities both vertically and horizontally in the model cells crossed by the ray paths.

We have based the addition of the fourth data set to our joint inversion code on the regional version of the double-difference (DD) tomography program *tomoDD* (Zhang and Thurber, 2003, 2006). DD tomography is a generalization of DD location (Waldhauser and Ellsworth, 2000) and it simultaneously solves for the 3D velocity structure and seismic event locations. DD tomography uses a combination of absolute and more accurate differential arrival times and hierarchically determines the velocity structure from larger scale to smaller scale. The differential times can be calculated from cross-correlation techniques for similar waveforms and by directly subtracting catalog arrival times for pairs of events at common stations.

The body-wave arrival time T from an earthquake i to a seismic station k is expressed using ray theory as a path integral,

$$T_k^i = \tau^i + \int_i^k uds \tag{1}$$

where τ^i is the origin time of event i, u is the slowness field, and ds is an element of path length. The source coordinates ($x1$, $x2$, $x3$), origin times, ray paths, and the slowness field are the unknowns. The relationship between the arrival time and the event location is highly nonlinear, so a truncated Taylor series expansion is generally used to linearize equation (1). This linearly relates the misfit between the observed and predicted arrival times r_k^i to the desired perturbations to the hypocenter and velocity structure parameters:

$$r_k^i = \sum_{l=1}^{3} \frac{\partial T_k^i}{\partial x_l^i} \Delta x_l^i + \Delta\tau^i + \int_i^k \delta uds. \tag{2}$$

Subtracting a similar equation for event j observed at station k from equation (2), we have

$$r_k^i - r_k^j = \sum_{l=1}^{3} \frac{\partial T_k^i}{\partial x_l^i} \Delta x_l^i + \Delta\tau^i + \int_i^k \delta uds - \sum_{l=1}^{3} \frac{\partial T_k^j}{\partial x_l^j} \Delta x_l^j - \Delta\tau^j - \int_j^k \delta uds. \tag{3}$$

Assuming that these two events are near each other so that the paths from the events to a common station are almost identical (Figure 1) and the velocity structure is known, then equation (3) can be simplified as

$$dr_k^{ij} = r_k^i - r_k^j = \sum_{l=1}^{3} \frac{\partial T_k^i}{\partial x_l^i} \Delta x_l^i + \Delta\tau^i - \sum_{l=1}^{3} \frac{\partial T_k^j}{\partial x_l^j} \Delta x_l^j - \Delta\tau^j, \tag{4}$$

where dr_k^{ij} is the so called double-difference (Waldhauser and Ellsworth, 2000) and equation (4) is known as the DD earthquake location algorithm. This term is the difference between observed and calculated differential arrival times for the two events and can also be written as

$$dr_k^{ij} = r_k^i - r_k^j = (T_k^i - T_k^j)^{obs} - (T_k^i - T_k^j)^{cal}. \tag{5}$$

TomoDD is built upon the double-difference location code hypoDD written by Waldhauser (2001). In the original *tomoDD* algorithm, an approximate pseudo-bending (ART-PB) ray-tracing algorithm (Um and Thurber, 1987) is used to find the rays and calculate the travel times between events and stations. The model is represented by velocity values specified on a regular set of 3-D nodes and the velocity values are interpolated by using the linear B-spline interpolation method. The hypocentral partial derivatives are calculated from the direction of the ray and the local velocity at the source (Lee and Stewart, 1981). The ray path is divided into a set of segments and the model partial derivatives are evaluated by apportioning the derivative to its eight surrounding nodes according to their interpolation weights on the segment midpoint (Thurber, 1983).

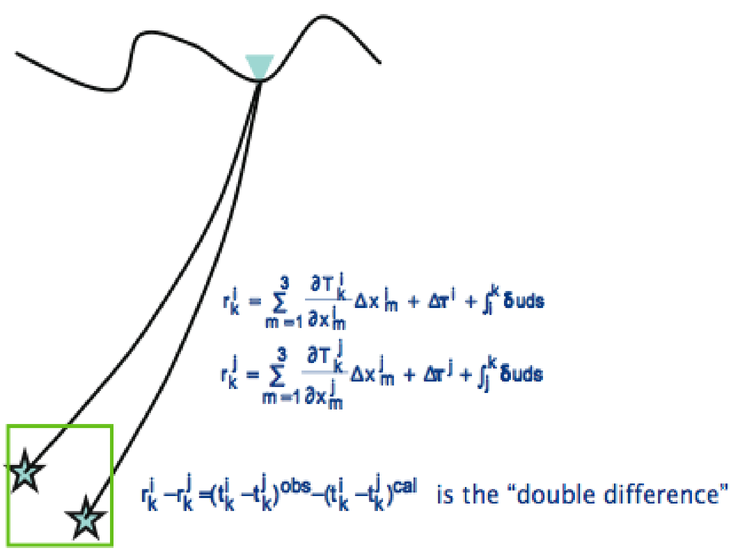

Figure 1. Sketch illustrating the DD concept for two close events (stars) recorded at the same station (triangle).

TomoDD assumes a flat earth model and is appropriate for local scale problems (10's to 100's of kilometers). At the regional scale (100's to 1000's of kilometers), however, sphericity of the earth should be taken into account. Major velocity discontinuities such as Conrad, Moho, and subducting slab boundary should also be considered. The ART-PB approach assumes a continuous velocity model and cannot deal properly with velocity discontinuities. For this reason and considering that our focus region of study is continental scale, we use the regional DD seismic tomography method (*tomoFDD*) that deals effectively with discontinuous velocity structures without knowing them a priori. *TomoFDD* uses a finite-difference method for determining travel times and ray paths, and treats the spherical Earth by embedding it (in part or in whole) within a Cartesian ''box''. *TomoFDD* uses a regular inversion grid.

Data

We will first conduct the proposed research in the Asian continent (in particular, between 20° N to 60° N latitude and 65° E to 140° E longitude) to then extend it to the whole Eurasia. We have obtained all gravity data for the full region of interest. These gravity observations were extracted from the global gravity model derived from the Gravity Recovery and Climate Experiment (GRACE) satellite mission (Tapley et al., 2005). These observations represent free-air gravity anomalies. Free-air gravity anomalies contain information not only of the subsurface density but also of topography. While in flat areas this may not represent a problem, in this region of great relief the topographic effect should be removed (Figure 2). Therefore, free-air gravity anomalies were converted into simple Bouguer gravity anomalies considering the standard density of 2670 kg/m^3.

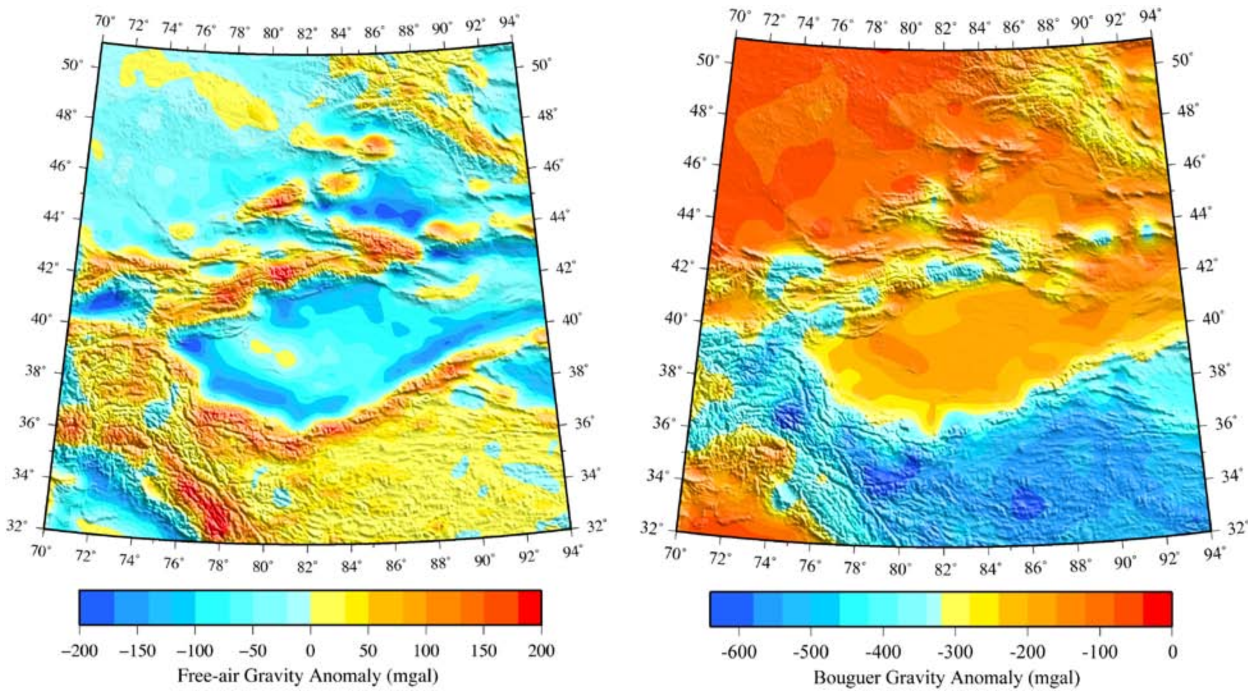

Figure 2. Gravity observations for the area surrounding the Tarim basin. (left) Free-air gravity anomalies extracted from the global gravity model derived from the GRACE satellite mission. Cold colors represent gravity lows meaning a mass deficit. Warm colors are gravity highs; (right) Bouguer gravity anomalies computed from the observations to the left.

We have obtained surface waves (Rayleigh and Love) dispersion observations for the Asian continent. These observations were generated considering the CUB (Colorado University at Boulder) surface wave tomographic models (Ritzwoller and Levshin, 1998; Levshin et al., 2001, 2002), and LANL Rayleigh wave slowness model (Maceira et al., 2005). In general, the tomographic patterns in these models (Figure 3) show a very good correlation with known geologic and tectonic features in the area.

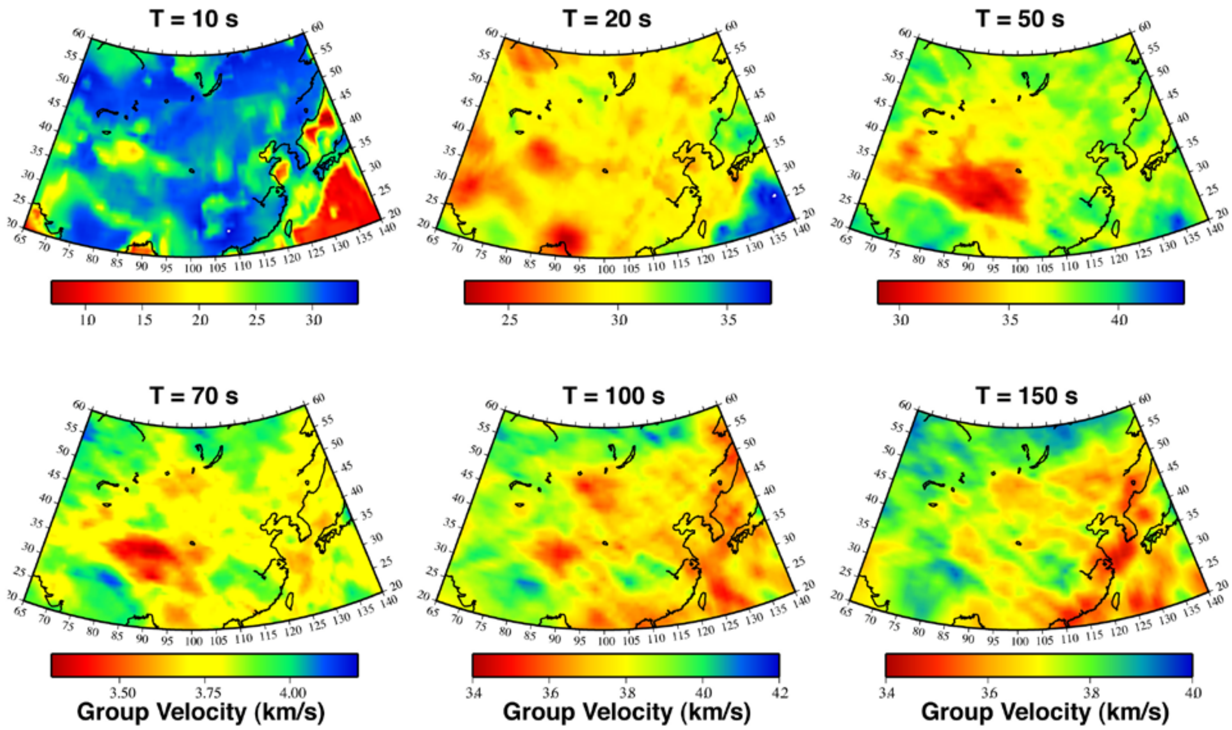

Figure 3. Fundamental mode Rayleigh wave group-velocity tomographic maps used to derive surface wave dispersion observations for each cell in our gridded model. Note that the color scale varies to preserve the details in each image.

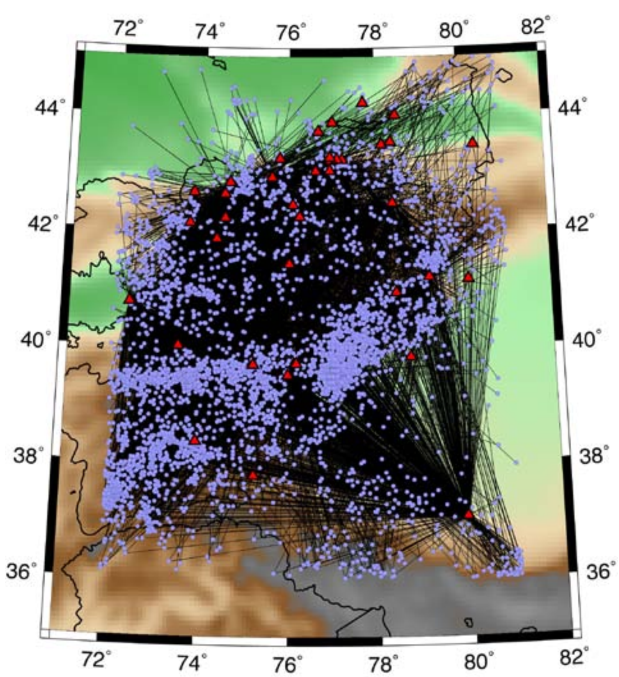

Figure 4. *S*-wave raypaths used for testing the joint inversion of 4 independent datasets. Red triangles are stations; blue dots are events.

The study area is seismically very active providing us with thousands of earthquakes recorded at regional and teleseismic distances. We have retrieved body wave travel time observations for 38 stations and 4,315 events in a small region in northwest China (Figure 4). These observations were retrieved from the LANL Knowledge Base. They represent a very small subset of all the available data and are being used to test the simultaneous joint inversion methodology of these 4 data sets.

We have obtained teleseismic *P*-wave receiver functions for 53 stations across the Asian continent. These observations were obtained via a joint Pennsylvania State University (PSU) and LANL effort (Ammon et al., 2004).

Preliminary results

We are testing the simultaneous joint inversion technique for the four datasets mentioned above in a small region that comprises the northwest corner of the Tarim basin. Figure 5 shows preliminary 3D shear wave velocity variations at constant depths of 5, 15, 27, and 52.5 km. Please note that the color scale is different for each depth slice.

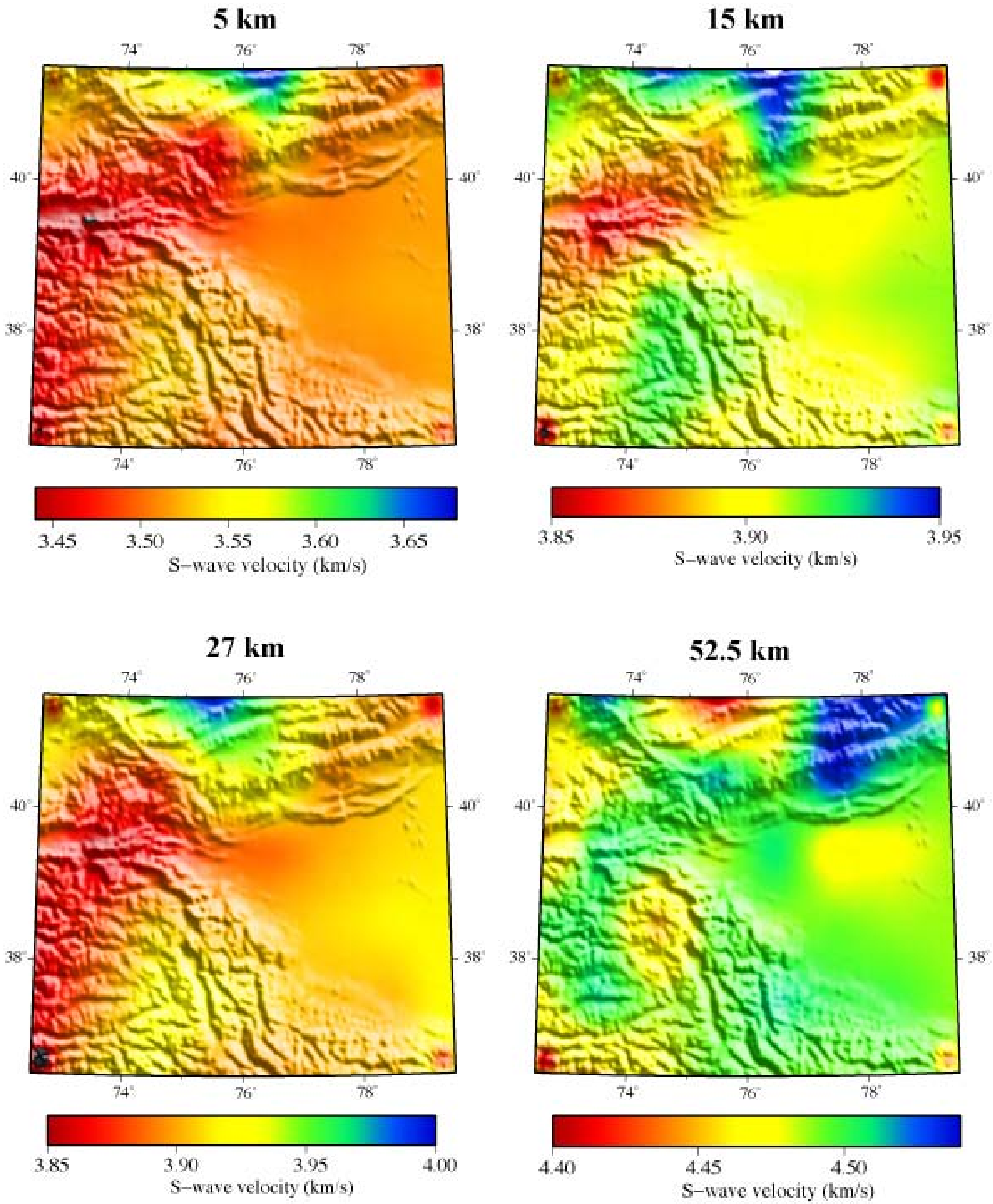

Figure 5. Preliminary *S*-wave velocity model at constant depth slices. The depth of each image is shown at the top of each map. Note the color scheme different for each image.

The results shown on Figure 5 are still preliminary and much work is still needed regarding the relative weighting of the four independent datasets as well as smoothing constrains and inclusion of *a priori* information into our inversion scheme.

Relations between seismic velocities and density

One of the difficulties with joint inversions is to determine a relationship between the independent data sets. In this case, we require constraints between seismic velocities and density. There is not a unique and universal relationship applicable to all types of lithologies at every single depth under all possible conditions of temperature and pressure. We are testing three different relationships between seismic velocities and density: (1) a combination of two existing empirical relationships; one more suitable for sedimentary rocks after Nafe and Drake (1963) and the well-known Birch's (1961) law more appropriate for basement rock; (2) Brocher's (2005); and (3) Harkrider's (see Acknowledgements). The testing area is a region in east Africa (Figure 5) where we have obtained on-land Bouguer gravity measurements (Ebinger et al., 1993; Tiberi et al., 2005) which we combine with LLNL surface wave tomographic models (Pasyanos and Nyblade, 2007). These sensitivity studies will ensure the validity of the relations used in our 3D seismic imaging efforts.

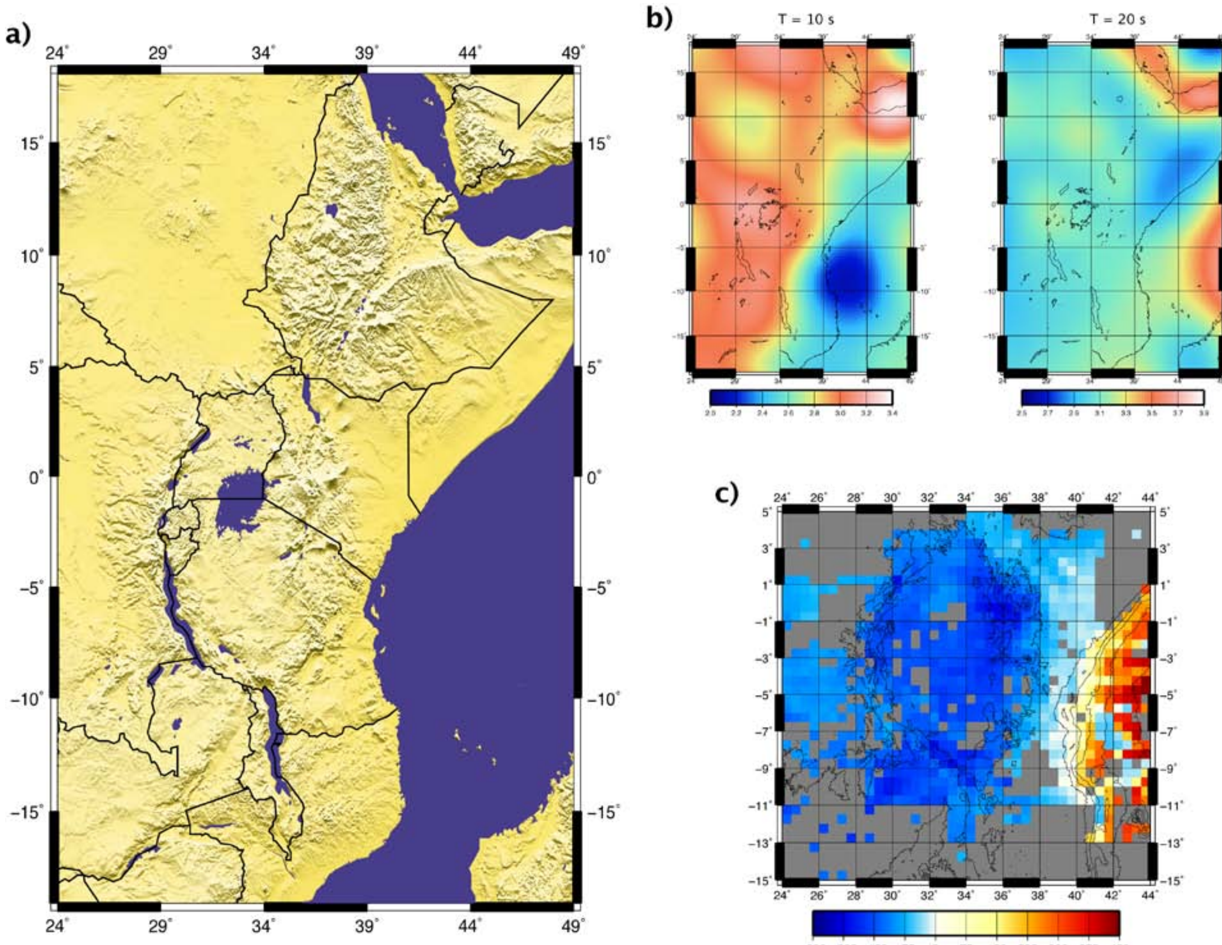

Figure 6. (a) Topographic map of East Africa; (b) Rayleigh wave group-velocity tomographic maps for the same area shown in (a) from Pasyanos and Nyblade (2007); (c) Bouguer gravity anomalies for the area under study from Ebinger et al. (1993).

CONCLUSIONS AND RECOMMENDATIONS

We have initiated a three-year project to map the three-dimensional (3D) seismic structure of the crust and upper mantle using seismic dispersion, gravity, receiver function, and travel time observations. 3D geophysical model development through the simultaneous inversion of complementary data sets to reduce uncertainty and bias is the future of 3D modeling. Geophysical models play an important role in Ground-based Nuclear Explosion Monitoring (GNEM). To more confidently and accurately detect, locate, and identify small seismic events, better high-resolution 3D structural models are needed. Therefore, the ongoing research directly addresses this challenge, and our results will also be of fundamental importance for understanding the geodynamic evolution and formation of continents, as well as the processes acting within and on the continental lithosphere.

We are first focusing on the Asian continent, an area of prime importance to NEM, and where we know there are adequate calibration events to validate our model and quantify its accuracy. We will then extend the modeling efforts to other regions including aseismic areas of interest to NEM.

Building on previous efforts, we have added body waves travel time observations to our simultaneous joint inversion technique. We now face the main challenge of relative weighting of the four independent datasets as well as smoothing constrains and inclusion of *a priori* information into our inversion scheme.

ACKNOWLEDGEMENTS

Special thanks to Cindy Ebinger for kindly providing us with her gravity measurements. We thank Anatoli Levshin, Michael Ritzwoller, and Mike Pasyanos for allowing us to use their tomographic maps for this research. Thanks also to Chuck Ammon for providing us with the receiver function observations. We thank the scientists, engineers, and technicians that have created the seismic recording systems and networks that provide excellent broad-band seismic observations. In particular, we thank the USGS and the IRIS Consortia (NSF) who share information and data with the global community in an effective and efficient manner. Thanks to Paul Wessel and Walter Smith for developing and maintaining their Generic Mapping Tool (GMT) that we use to create many of the illustrations used in our research. Many thanks to David Harkrider for valuable information gleaned from personal communication. Finally, our thanks to Jody Benson and Marv Wetovsky for editorial assistance.

REFERENCES

Aki, K., A. Christoffersson, and E. S. Husebye (1977). Determination of the three-dimensional seismic structure of the lithosphere, *J. Geophys. Res*. 82: 277–296.

Ammon, C. J., W. Sevilla, R. B. Herrmann, and G. E. Randall (2004). Systematic inversion of receiver functions and surface wave dispersion for crustal structure in central Asia, in *Proceedings of the 26th Seismic Research Review: Trends in Nuclear Explosion Monitoring*, LA-UR-04-5801, Vol.1, pp. 29–38.

Birch, F. (1961). The velocity of compressional waves in rocks to 10 kilobars, part 2, *J. Geophys. Res*. 66: 2199– 2224.

Brocher, T. M. (2005). Empirical relations between elastic wavespeeds and density in the Earth's crust, *Bull. Seismol. Soc. Am.* 95: 2081–2092.

Ebinger, C. J., A. L. Deino, A. L. Tesha, T. Becker, and U. Ring (1993). Tectonic controls on rift basin morphology: Evolution of the northern Malawi (Nyasa) rift, *J. Geophys. Res*. 98: 17821–17836.

Huang, Z., W. Su, Y. Peng, Y. Zheng, and H. Li (2003). Rayleigh wave tomography of China and adjacent regions, *J. Geophys. Res*. 108: doi:10.1029/2001JB001696.

Julià, J., C. J. Ammon, R. B. Herrmann, and A. M. Correig (2000). Joint inversion of receiver function and surface wave dispersion observations, *Geophys. J. Int*. 143: 99–112.

Julià, J., C. J. Ammon, and R. B. Herrmann (2003). Lithospheric structure of the Arabian shield from the joint inversion of receiver functions and surface wave dispersion, *Tectonophysics,* 371: 1–21.

Julià, J., C. J. Ammon, and A. A. Nyblade (2005). Evidence for mafic lower crust in Tanzania, East Africa, from joint inversion of receiver functions and Rayleigh wave dispersion velocities, *Geophys. J. Int.* 162: 555–569.

Jupp, D. L. B, and K. Vozoff (1975). Stable iterative methods for the inversion of geophysical data, *Geophys. J. R. Astr. Soc*. 42: 957–976.

Lee, W. H. K., and S. W. Stewart (1981). Principles and applications of microearthquake networks, *Adv. Geophys. Suppl.* 2, 293 pp.

Lees, J. M., and J. C. VanDecar (1991). Seismic tomography constrained by Bouguer gravity anomalies: Applications in western Washington, *Pure and Appl. Geophys*. 135: 31–52.

Levshin, A. L., M. H. Ritzwoller, M. P. Barmin, and J. L. Stevens (2001). Short period group velocity measurements and maps in central Asia, in *Proceedings of the 23rd Seismic Research Review: Worldwide Monitoring of Nuclear Explosions*, LA-UR-01-4454, Vol. 1, pp. 258–269.

Levshin, A. L., J. L. Stevens, M. H. Ritzwoller, and D. A. Adams (2002). Short-period (7-s to 15-s) group velocity measurements and maps in central Asia, in *Proceedings of the 24th Seismic Research Review—Nuclear Explosion Monitoring: Innovation and Integration,* LA-UR-02-5048, Vol. 1, pp. 97–106.

Lines, L. R., A. K. Schultz, and S. Treitel (1988). Cooperative inversion of geophysical data, *Geophysics* 53: 8–20.

Maceira, M. and C. J. Ammon (2009). Joint inversion of surface wave velocity and gravity observations and its application to Central Asian basins shear velocity structure, *J. Geophys. Res*. 114: B02314, doi:10.1029/2007JB005157.

Maceira, M. and C. J. Ammon (2006). Joint inversion of surface wave velocity and gravity observations and its application to Central Asian basins shear velocity structure, *Seismol. Res. Lett*. 77: 2, 297.

Maceira, M., S. R. Taylor, C. J. Ammon, X. Yang, and A.A. Velasco (2005). High Resolution Rayleigh Wave Slowness Tomography of Central Asia, *J. Geophys. Research*., 110: No. B6, B06304, doi:10.1029/2004JB003429.

Nafe, J. E., and C. L. Drake (1963). Physical properties of marine sediments, in *The Sea*, vol. 3, edited by M. N. Hill, pp. 794–815, Interscience, New York.

Onizawa, S., H. Mikada, H. Watanabe, and S. Sakashita (2002). A method for simultaneous velocity and density inversion and its application to exploration of subsurface structure beneath Izu-Oshima volcano, Japan, *Earth Planets Space* 54: 803–817.

Oppenheimer, D. H., and K. E. Herkenhoff (1981). Velocity-density properties of the lithosphere from three-dimensional modeling at the Geysers-Clear Lake region, California, *J. Geophys. Res*. 86: 6057–6065.

Parsons, T., R. J. Blakely, and T. M. Brocher (2001). A simple algorithm for sequentially incorporating gravity observations in seismic traveltime tomography, *International Geol. Rev*. 43: 1073–1086.

Pasyanos, M. E., and A. A. Nyblade (2007). A top to bottom lithospheric study of Africa and Arabia, *Tectonophys.* 444: 27–44.

Ritzwoller, M. H. and A. L. Levshin (1998). Eurasian surface wave tomography: group velocities, *J. Geophys. Res.* 103: 4839–4878.

Rowe, C. A., W. S. Phillips, M. Maceira, M. Begnaud, L. Steck, X. Yang, C. Lucero, H. Hartse, R. Stead, K. Mackey, K. Fujita, and C. Ammon (2007). Geophysical Imaging of Asia and Siberia: Tomograhy for Seismic Velocity, Upper Mantle Gradient, Lg Attenuation, and Joint Inversion of Surface Wave Dispersion, Receiver Functions and Satellite Gravity Data, in *Proceedings of the 29th Monitoring Research Review: Ground-Based Nuclear Explosion Monitoring Technologies*, LA-UR-07-5613, Vo. 1, pp. 256–265.

Tapley, B., et al. (2005). GGM02 - An improved Earth gravity field model from GRACE, *J. Geodesy*, DOI 10.1007/s00190-005-0480-z.

Tiberi, C., C. Ebinger, V. Ballu, G. Stuart, and B. Oluma (2005). Inverse models of gravity data from the Red Sea-Aden–East African rifts triple junction zone, *J. Geophys. Int*. 163: 775–787.

Thurber, C. H. (1983). Earthquake locations and three-dimensional crustal structure in the Coyote Lake area, central California, *J. Geophys. Res.* 88: 8226–8236.

Um, J., and C. H. Thurber (1987). A fast algorithm for two-point seismic ray tracing, Bull. Seism. Soc. Am. 77: 972–986.

Villaseñor, A., M. H. Ritzwoller, A L. Levshin, M. P. Barmin, E. R. Engdahl, W. Spakman, and J. Trampert (2001). Shear velocity structure of central Eurasia from inversion of surface wave velocities, *Phys. Earth Planet. Inter.* 123: 169–184.

Waldhauser, F. (2001). hypoDD: a computer program to compute double difference hypocenter locations, *U.S. Geol. Surv. Open File Rept. 01-113*, 25 pp.

Waldhauser, F., and W. L. Ellsworth (2000). A double-difference earthquake location algorithm: method and application to the northern Hayward Fault, California, *Bull. Seism. Soc. Am.* 90: 1353–1368.

Zhang, H., and C. Thurber (2006). Development and applications of double-difference tomography, *Pure and Applied Geophys.*, 163, 373-403, doi:10.1007/s00024-005-0021-y.

Zhang, H., and C. H. Thurber (2003). Double-Difference Tomography: The Method and Its Application to the Hayward Fault, California, *Bull. Seism. Soc. Am*. 93: 1875–1889.